Leveraging Zone Air Temperature Data to Improve Physics-Based Energy Simulation of Existing Buildings

Sang Hoon Lee[1], Tianzhen Hong[1]

[1]Lawrence Berkeley National Laboratory, Berkeley, United States

Abstract

The paper introduces a hybrid modelling approach that enhances the accuracy and usability of physics-based energy simulation for existing buildings. The approach leverages measured zone air temperature data streams—increasingly available from smart thermostats—to derive difficult-to-obtain input parameters for internal thermal mass and infiltration airflow rates. It does so using a reformulated inverse heat balance algorithm. We implemented the inverse algorithms in EnergyPlus and used LBNL's Facility for Low Energy eXperiments (FLEXLAB) for demonstration and validation.

Introduction

Building energy retrofits are a cost effective means of achieving greenhouse gas emissions reductions by improving energy efficiency. Retrofit projects often rely on energy simulation to quantify energy savings from energy conservation measure (ECM) packages and serve as the basis for project financial calculations. However, energy simulation requires several inputs that are not easy to collect, leading to uncertainty in energy savings estimates, and increasing project risk (Lee et al. 2015; Hong et al. 2015).

There are two common approaches to energy modelling: data-driven "black-box", and physics-based "white-box" (ASHRAE 2013). The data-driven approach uses measured data and various statistical and inverse modelling techniques to develop models that take arbitrary collections of input variables (Zhang et al. 2015). Data-driven models tend to be both application specific *and* building specific, with some applications requiring significant amounts of measured data for training purposes. These characteristics make data-driven models difficult to scale up to be applied to different buildings.

Physics-based approaches cover a wide spectrum of complexity from low-fidelity reduced order and steady-state models (ISO 2008; Cole et al. 2014; Kokogiannakis, Strachan, and Clarke 2008) to high fidelity, dynamic models (Clarke 2001; Hunn 1996; DOE 2015). Decades of research have brought development of various energy modelling methods and reviews of them (Hong, Chou, and Bong 2000; Augenbroe 2002; Zhao and Magoulès 2012), offering many calculation tools (Crawley et al. 2008). Whereas physics-based models are general with respect to both buildings and applications, their drawback is that they require a significant number of building input parameters, some of which are quite difficult to obtain in practice.

Two significant, yet difficult-to-obtain input parameters for physics-based models are internal thermal mass and infiltration rate. Internal thermal mass refers to non-structural elements with thermal capacitance such as changeable partitions, furniture, and books. Although internal thermal mass has substantial influence on peak cooling and heating requirement calculations, it has not been well highlighted in building energy simulation practice because it is both difficult to measure in compact form (e.g., a thermal mass constant for a zone) and difficult and time-consuming to characterize in more granular form (e.g., mass and thermal properties of furniture and books) (Zeng et al. 2011; Wang and Xu 2006). Infiltration is similarly difficult to measure and characterize. Blower door testing is not applicable to commercial buildings. Specifying the sizes and distribution of cracks in the building envelope, the permeability of the envelope, the airflow to the building, and the pressure distribution in and around the building is impractical. Infiltration rates also change in time and dynamically interact with indoor and outdoor temperature, wind speed, and HVAC operation. Energy simulation engines use compact inputs for internal thermal mass and infiltration. However, high uncertainty in these parameters propagate to simulation results and negatively impact retrofit analysis.

Model input calibration uses measured data to improve physics-based model inputs. The challenge in calibration is that physics-based models have many uncertain input parameters and that many combinations of values for those parameters can match measured data. Significant domain expertise is required to determine which parameter modifications correspond to physical conditions.

This paper explores a hybrid approach that combines inverse and forward methods to essentially perform *targeted* calibration on specific inputs. We develop selectively inverse heat balance algorithms that leverage widely available space temperature data from smart thermostats to extract values for infiltration and internal thermal mass. Once extracted, these inputs are used in the conventional forward-only physics-based simulation. Figure 1 illustrates the concept. Whereas conventional calibration uses an unmodified simulation engine and multiple runs to tune multiple input parameters, hybrid

modelling uses a single run of a modified simulation engine to tune selected parameters.

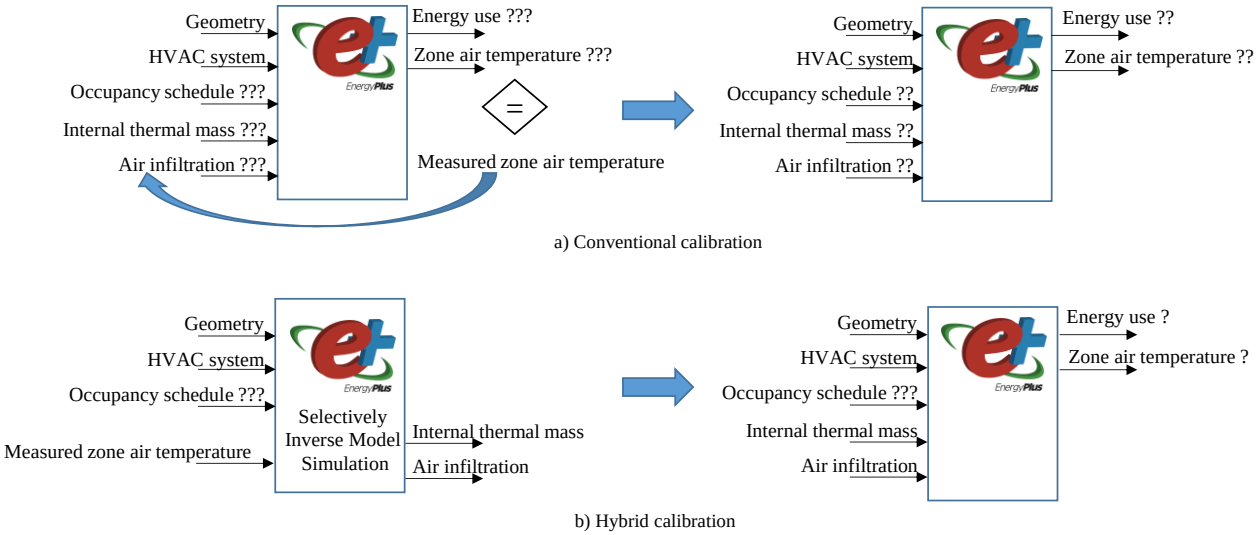

Figure 1 Hybrid approach that integrates forward and inverse modelling methods to calibrate targeted model inputs (? slightly unknown, ?? some unknown, ??? very unknown)

In this paper, we derive inverse heat balance algorithms for internal thermal mass and infiltration. We describe an implementation in EnergyPlus as well as demonstration and validation experiments using the LBNL's Facility for Low Energy eXperiments (FLEXLAB)(LBNL 2016).

Approach and Implementation

We developed and implemented the selectively inverse heat balance algorithms in EnergyPlus, DOE's open-source whole-building energy simulation engine (DOE 2016). A new EnergyPlus object HybridModel:Zone defines inputs for the model. The object specifies calculation options, a measured temperature data input Schedule:File object, and the temperature measurement period. These are defined on a per zone basis.

HybridModel:Zone,

A1, \field Name
A2, \field Zone Name
A3, \field Calculate Zone Internal Thermal Mass (Yes or No)
A4, \field Calculate Zone Air Infiltration Rate (Yes or No)
A5, \field Zone Measured Air Temperature Schedule Name
N1, \field Begin Month
N2, \field Begin Day of Month
N3, \field End Month
N4; \field End Day of Month

Nomenclature

Q_{int}	Internal heat gain
h_s	Convective heat transfer coefficient
A_s	Zone surface area
T_s	Zone surface temperature
T_z	Zone air temperature
T_{iz}	Interzone air temperature
T_o	Outdoor air temperature
T_{sup}	Air system supply air temperature
q_{inf}	Infiltration air flow rate
$\dot{m}_{iz}$	Interzone air mass flow rate
$\dot{m}_{sys}$	Air system mass flow rate
V	Zone volume
ρ_{air}	Air density
C_z	Heat capacity of zone air and internal thermal mass
C_p	Zone air specific heat
C_T	Heat capacity multiplier
A	Constant coefficient
B	Temperature coefficient
C	Velocity coefficient
D	Velocity squared coefficient
v_{wind}	Wind velocity
$F_{schedule}$	Infiltration schedule value between 0 and 1

Inverse heat balance approach

Our approach begins with the fundamental physics-based zone air heat balance algorithm shown in following equations.

$$C_z \frac{dT_z}{dt} = \sum Q_{int} + \sum h_s A_s (T_s - T_z) + \sum \dot{m}_{iz} C_p (T_{iz} - T_z) + \dot{m}_{inf} C_p (T_o - T_z) + Q_{sys} \quad (1)$$

The energy stored in the zone is the product of zone temperature T_z and zone heat capacitance C_z. Equation (1)

calculates the change in zone energy—the change in zone temperature—as the sum of zone loads and the energy provided by the HVAC system Q_{sys}. C_z includes both zone air and internal thermal mass, which is assumed to be in thermal equilibrium with zone air. The infiltration mass flow rate is $\dot{m}_{inf}$.

Our approach selectively inverts Equation (1) and uses zone temperature data streams—zone temperature differences or dT_z/dt to calculate C_z and $\dot{m}_{inf}$.

EnergyPlus has two zone air heat balance solution algorithms: 3rd order backward difference and analytical. The 3rd order finite difference approximation provides stability without requiring a prohibitively small time step, but has truncation errors and requires a fixed time step length for the previous three time steps. Therefore, different time step lengths may result in invalid temperature coefficients. The analytical algorithm is an integration approach that can obtain solutions without truncation errors. It also requires zone air temperature for the previous time step only and is thus independent of time step length.

Inverse model for internal thermal mass

There are two approaches to model internal thermal mass in EnergyPlus: InternalMass objects and zone heat capacitance multipliers.

The InternalMass object specifies construction materials and surface areas of internal mass objects. InternalMass objects participate in zone air heat balance and long-wave radiant exchange, and exchange energy through its both surfaces by convection. The geometry of InternalMass objects is greatly simplified. They do not directly interact with solar heat gain calculations because they do not have a specific location in space.

The ZoneCapacitanceMultiplier:ResearchSpecial object is an alternative compact specification that sidesteps challenges in determining volumes and thermal properties of individual internal thermal mass objects. Shown in Equation (2), the capacitance multiplier C_T scales the heat capacity of the air in the zone. A value of 1.0 indicates the capacitance comes only from zone air.

The zone capacitance multiplier only corrects the zone air heat capacity reflecting heat stored in the internal mass. Assumptions are not different from the approach used in the InternalMass object, which ignores the geometry construction of the internal mass, and does not receive the solar heat gain through windows.

EnergyPlus assumes a single constant multiplier for all zones (DOE 2015). Although users can set this multiplier, it is not easy to determine a reasonable value for a typical or specific room furniture configuration. We enhance EnergyPlus to allow zone-specific multipliers.

Inverse algorithm for zone capacitance multiplier

The inverse model derives the zone capacitance multiplier C_T. The formulation starts with the zone-air heat balance. Equation (2) calculates the time-series zone air temperature T_z by solving Equation (1) using the analytical solution method.

Equation (3) inverts Equation (2), replacing calculated zone air temperature T_z with the measured zone air temperatures for the current time step T_z^t and the previous time step $T_z^{t-\delta t}$. It calculates the time step zone air heat capacity C_z^t.

Equation (3) is only solved when the HVAC system is off. When the HVAC system is operating, the zone temperature is maintained at the setpoint temperature, thus the temperature difference between T_z^t and $T_z^{t-\delta t}$ is zero (or near zero), and the denominator of Equation (3) becomes zero too.

The model determines a time span when $|T_z^t - T_z^{t-\delta t}| > 0.05°C$ that provides a more stable condition to determine C_z^t. Internal mass multiplier calculations are only done when the zone air temperature difference between two adjacent time steps meets the condition. This filter is needed for more reliable inverse calculation to avoid the anomaly conditions due to the use of the inverse model.

The temperature capacitance multiplier, i.e., internal mass multiplier, C_T^t is calculated for each time step using Equation (4).

Inverse model for infiltration

Infiltration rates used in energy modelling rarely reflect actual building operating conditions, as they are both dynamic and difficult to measure. Infiltration rate is a function of building age, construction quality, and weather. Wind speed and outdoor temperature at zone height—both are sensitive to elevation and height from the ground—affect pressure difference between the outside and the inside of a building, and therefore infiltration.

The EnergyPlus ZoneInfiltration:DesignFlowRate object defines a base infiltration flow rate and coefficients for temperature and wind velocity. EnergyPlus calculates airflow rates by adjusting for indoor-outdoor temperature differences and outdoor wind speed using Equation (5).

A constant infiltration flow rate is designed to capture the average effect over the year and in different locations. The simple infiltration approach has an empirical correlation that modifies the infiltration as a function of wind speed and temperature difference across the envelope. The difficulty in using this approach is the determination of valid coefficients for each building type in each location.

Infiltration inverse algorithm

It is not easy to estimate and characterize various sources of infiltration as well as factors affecting infiltration. The inverse model addresses this difficulty by deriving the infiltration airflow rate $\dot{m}_{inf}$ directly. Again, we reformulate the zone air heat balance algorithm. The time-series zone air temperature, T_z using the 3rd order method is shown in Equation (6). Equation (7) shows the inverse algorithm to derive the zone infiltration mass flow rate using the measured zone air temperature. The infiltration airflow, q_{inf} is then calculated from the derived infiltration mass flow rate from the Equation (8). The inverse equation derives more reliable infiltration airflow rates for time steps when the zone air temperature

difference between adjacent time steps is small, so that the internal thermal mass term (an unknown) can be ignored.

$$T_z^t = \left(T_z^{t-\delta t} - \frac{\sum Q_{int} + \sum h_s A_s T_s + \sum \dot{m}_{iz} C_p T_{iz} + \dot{m}_{inf} C_p T_o + \dot{m}_{sys} C_p T_{sup}^t}{\sum h_s A_s + \sum \dot{m}_{iz} C_p + \dot{m}_{inf} C_p + \dot{m}_{sys} C_p}\right) \times e^{\left(-\frac{\sum h_s A_s + \sum \dot{m}_{iz} C_p + \dot{m}_{inf} C_p + \dot{m}_{sys} C_p}{C_z^t}\delta t\right)} + \frac{\sum Q_{int} + \sum h_s A_s T_s + \sum \dot{m}_{iz} C_p T_{iz} + \dot{m}_{inf} C_p T_o + \dot{m}_{sys} C_p T_{sup}^t}{\sum h_s A_s + \sum \dot{m}_{iz} C_p + \dot{m}_{inf} C_p + \dot{m}_{sys} C_p} \quad (2)$$

$$C_z^t = -\frac{\left(\sum h_s A_s + \sum \dot{m}_{iz} C_p \dot{m}_{inf} C_p + \dot{m}_{sys} C_p\right)\delta t}{ln\left[\frac{T_z^t - \frac{\sum Q_{int} + \sum h_s A_s T_s + \sum \dot{m}_{iz} C_p T_{iz} + \dot{m}_{inf} C_p T_o + \dot{m}_{sys} C_p T_{sup}^t}{\sum h_s A_s + \sum \dot{m}_{iz} C_p + \dot{m}_{inf} C_p + \dot{m}_{sys} C_p}}{T_z^{t-\delta t} - \frac{\sum Q_{int} + \sum h_s A_s T_s + \sum \dot{m}_{iz} C_p T_{iz} + \dot{m}_{inf} C_p T_o + \dot{m}_{sys} C_p T_{sup}^t}{\sum h_s A_s + \sum \dot{m}_{iz} C_p + \dot{m}_{inf} C_p + \dot{m}_{sys} C_p}}\right]} \quad (3)$$

$$C_T^t = \frac{C_z^t}{V \rho_{air} C_p} \quad (4)$$

$$q_{inf} = q_{inf\_design} F_{schedule}[A + B|T_z - T_o| + C \times v_{wind} + D \times (v_{wind})^2] \quad (5)$$

$$T_z^t = \frac{\sum Q_{int} + \sum h_s A_s T_s + \sum \dot{m}_{iz} C_p T_{iz} + \dot{m}_{inf} C_p T_o + \dot{m}_{sys} C_p T_{sup}^t - (\frac{C_z}{\delta t})(-3T_z^{t-\delta t} + \frac{3}{2}T_z^{t-2\delta t} - \frac{1}{3}T_z^{t-3\delta t})}{\left(\frac{11}{6}\right)\frac{C_z}{\delta t} + \sum h_s A_s + \sum \dot{m}_{iz} C_p + \dot{m}_{inf} C_p + \dot{m}_{sys} C_p} \quad (6)$$

$$\dot{m}_{inf} = \frac{\sum Q_{int} + \sum h_s A_s T_s + \sum \dot{m}_{iz} C_p T_{iz} + \dot{m}_{sys} C_p T_{sup}^t - \left(\frac{C_z}{\delta t}\right)\left(-3T_z^{t-\delta t} + \frac{3}{2}T_z^{t-2\delta t} - \frac{1}{3}T_z^{t-3\delta t}\right) - T_z^t\left(\left(\frac{11}{6}\right)\frac{C_z}{\delta t} + \sum h_s A_s + \sum \dot{m}_{iz} C_p + \dot{m}_{sys} C_p\right)}{C_p(T_z^t - T_o)} \quad (7)$$

$$q_{inf} = \frac{\dot{m}_{inf}}{\rho_{air}} \quad (8)$$

The calculation is only activated when the zone air temperature difference between the current and previous time step is less than 0.05°C, and the zone air and outdoor air temperature difference is greater than 5 °C, i.e., $|T_z^t - T_o^t| > 5.0\,°C$ and $|T_z^t - T_z^{t-\delta t}| < 0.05°C$.

Model Validation Using Simulated Data

We validated the hybrid approach using both simulation and physical measurement. We used simulation to show that the inverse heat balance algorithm can correctly recover known values for internal thermal mass and infiltration when other input parameters are known.

We used an EnergyPlus model to generate ten-minute interval zone air temperature data and then fed the data to EnergyPlus operating in the hybrid mode to recover the original infiltration airflow rates and internal mass multipliers. The results are shown in Table 1 for a variety of thermal mass and infiltration configurations.

Inversely derived infiltration values match original input values closely. Derived internal mass multipliers showed about 20% of deviation from the original input values.

Model Validation Using Measured Data

LBNL's FLEXLAB allows testing of building systems individually or as an integrated system under real-world conditions for flexible, comprehensive, and advanced experiments (LBNL 2016). The facility comprises four testbeds, each with two identical thermally isolated cells. Cells are heavily instrumented and monitor the performance of HVAC systems, lighting, windows, building envelope, control systems, and plug loads.

Figure 2 Exterior view of the FLEXLAB testbed Cell 3A

FLEXLAB experimental setup

Our experiment used the FLEXLAB testbed cell 3A (Figure 2) for 50 days from April 4 to May 23, 2016.

Accurate measurement of indoor air temperature under various infiltration airflow rates and internal mass configurations was critical for validation of the inverse heat balance algorithms. Four stratification sensor trees were located at the central points of the cell. Each tree has seven temperature sensors placed at equal intervals from floor to the ceiling. We collected temperature data at one-minute intervals, storing them in an sMAP (Simple Measurement and Actuation Profile) system (Dawson-Haggerty et al. 2010). We used controlled internal heat gains representing a typical office setting: 21 W/m^2 (2 W/ft^2) between 8am and 6pm and 0 during other hours (Deru et al. 2011). Air mixing fans operated continuously to ensure well mixing of zone air. The HVAC system was turned off for the entire experiment.

We experimented with a range of interior mass and infiltration configurations. A Light mass (LM) configuration used six sets of light-mass desks, chairs, cotton manikins, desktop computers, and monitors (Figure 3). A Heavy mass (HM) configuration added about 1000 library books in 50 boxes (Figure 4).

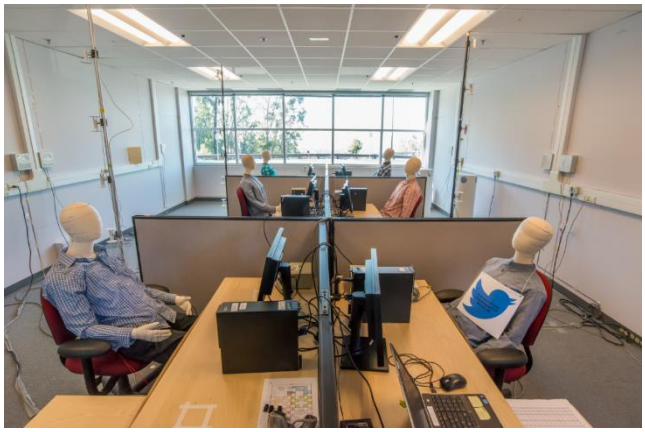

Figure 3 Experiment cell space with an office configuration representing light internal thermal mass

Figure 4 Experiment cell with about 1000 added books representing heavy internal thermal mass

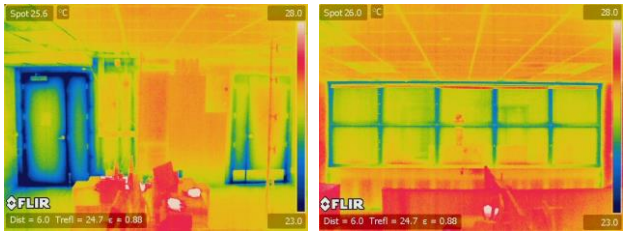

Figure 5 Infrared images of the entrance door and mechanical closet door (left), and windows (right)

We used forward EnergyPlus simulations to empirically determine that the zone capacitance multipliers corresponding to these two configurations were 3.0 and 5.0, respectively. For infiltration air flow rates, we used four settings, Inf1: a tight configuration case of 0.1 ACH (air changes per hour), the natural cell condition with doors, windows, and air dampers closed; Inf2: a medium infiltration configuration of 0.42 ACH, Inf3: a high infiltration configuration with 2.0 ACH, and Inf4: infiltration with a schedule, 0.18 ACH 6am–10pm and 0.7 ACH 10pm–6am. We installed a fan to control the amount of the exhaust air, which would introduce the same amount of the outdoor air through the supply duct with an open damper and the door and window gap. We used CO_2 tracer gas decay testing (ASTM 2011; ISO 2012) to measure the air change in the testbed. Figure 5 shows infrared images of the experimental cell. The left image shows significant heat transfer from the direct infiltration through the entrance door gap. The right image shows that the door of the mechanical closet introduces unwanted cold air into the cell, a significant heat loss. The experiment recorded sensor data for energy model calibration and model validation. The sensor data include:

- Zone air temperature from 28 sensors (four stratification trees, each with seven sensors). The average temperature from 20 sensors is used as the zone air temperature data. The top (underneath the ceiling tile) and bottom (above the floor) temperature sensors for each stratification tree were excluded from the average calculation.
- Electric power from individual outlets for electric heaters, air mixing fans, exhaust air fan, and control systems (computers, sensor connection hubs).
- CO_2 PPM decay data for each zone infiltration case.
- Outside air inlet temperature from the supply air duct.
- Internal wall surface temperature.
- Floor slab temperature.
- Outdoor air dry-bulb temperature, global solar irradiation, solar diffuse radiation, and wind speed.

Validation results

Zone air heat capacity needs to be derived from the stabilized internal zone air temperature data that fully captures the stored heat in the air and internal thermal mass. Measured temperature data was limited to only three days for each case. To overcome the data limitation, four days of simulated temperature data, from the calibrated model, were added to the dataset. This is based

on simulation runs that show seven days is needed to reach stabilized indoor conditions for each configuration changes at the FLEXLAB environment. Figure 6 presents the calculated infiltration and internal mass multipliers at each time step. The rectangular box in the chart indicates for three days of the inverse model simulation using the measured temperature. There is noise in the calculated infiltration airflow rates and internal mass multipliers for the period where the measured zone air temperature data were used. Although the calibrated model reflects the dynamics of the indoor environment as represented in the measured air temperature, small differences in zone air temperature creates uncertainties in the model parameters.

Discussion

Empirical validation using FLEXLAB underscores the importance of longer temperature data streams for deriving internal thermal mass. Because internal thermal mass stabilizes zone temperatures, longer data periods are needed to capture the thermal inertia. Seven days of data are recommended.

Table 1 Calculated infiltration and internal mass multiplier using the simulated zone air temperature

	Infiltration (ACH)				***Internal Mass Multiplier***			
	Energy Model Input	Calculated using ***Simulated*** Air Temperature			Energy Model Input	Calculated using ***Simulated*** Air Temperature		
		2 months average	1 week average	3 days average		2 months average	1 week average	3 days average
LM_Inf1	0.10	0.10	0.10	0.10	3.00	3.22	3.25	3.30
LM_Inf2	0.42	0.42	0.42	0.42	3.00	3.27	3.34	3.58
LM_Inf3	2.00	2.00	2.00	2.00	3.00	3.51	3.53	3.55
LM_Inf4	0.7 nighttime, 0.18 daytime	0.7 nighttime, 0.17 daytime	0.7 nighttime, 0.18 daytime	0.7 nighttime, 0.18 daytime	3.00	3.19	3.23	3.32
HM_Inf1	0.10	0.10	0.10	0.10	5.00	5.29	5.26	5.21
HM_Inf2	0.42	0.42	0.42	0.42	5.00	5.28	5.24	5.18
HM_Inf3	2.00	2.00	2.00	2.00	5.00	5.56	5.51	5.41
HM_Inf4	0.7 nighttime, 0.18 daytime	0.7 nighttime, 0.17 daytime	0.7 nighttime, 0.17 daytime	0.7 nighttime, 0.17 daytime	5.00	5.21	5.18	5.09

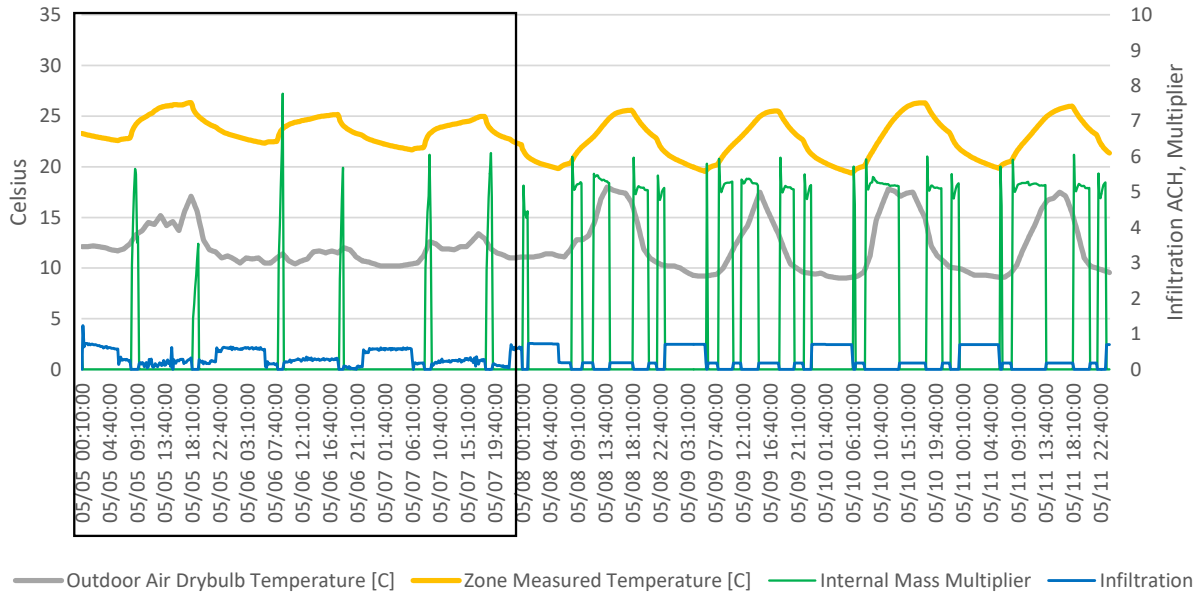

Figure 6 HybridModel simulation results indicating time step infiltration and internal mass multiplier for the experiment case of the office configuration with books and the scheduled infiltration

The internal mass validation study using the DOE reference energy models (Deru et al. 2011) shows that a multiplier of 8.0 reflects a typical office configuration. An internal mass multiplier of 3 to 6 is recommended for light offices, 6 to 10 for typical offices, and 10 to 15 for heavy mass office configurations. When both the infiltration and internal mass parameters are unknown, they cannot be solved analytically using only one known zone air temperature. The problem can be formulated as an optimization problem that can be solved using iterative process.

For example, the infiltration hybrid model simulation comes first with an assumption of a default internal mass multiplier (we recommend to use 8) representing a typical office furnishing configuration. Then the calculated infiltration can be used to adjust the internal mass multiplier by running the hybrid model simulation. This iterative process ends when satisfied solutions are achieved. This mode of hybrid modelling needs further research.

The accuracy of the inverse model is dependent on the completeness of—and lack of uncertainty in—the energy model. Other uncertain parameters will influence the infiltration and internal mass multipliers because multiple combinations of the parameter values can match the measured zone air temperature. Uncertainty should be minimized using on-site actual weather data. Future research is needed to investigate how the inverse model can be integrated with the traditional model calibration process.

Conclusions

The paper presents a hybrid energy modelling approach that combines forward and inverse physics-based modelling. The approach uses measured zone air temperature data—increasingly available from smart thermostats—to replace traditionally difficult to obtain parameters for internal thermal mass and infiltration airflow rate. It does so by reformulating and selectively inverting the zone air heat balance algorithm.

We implemented the hybrid model in EnergyPlus and tested it using both traditional forward-only simulation and empirical data obtained from LBNL's FLEXLAB. Experiments show good agreement between parameters for internal thermal mass and infiltration airflow rates and values derived using the HybridModel feature.

The HybridModel feature will be available in the spring 2017 EnergyPlus 8.7 release. It will enable more accurate energy performance assessments of and predictions for existing buildings, supporting better energy-efficiency retrofit decision making.

Acknowledgment

This work was supported by the 2014 Building Energy Efficiency Frontiers and Incubator Technologies Program of the United States Department of Energy. The authors wish to recognize Amir Roth, Technology Manager of the Building Technologies Office of the US Department of Energy, for his support and assistance in this work.

References

ASHRAE. 2013. *ASHRAE Handbook: Fundamentals 2013*.

ASTM. 2011. *Standard Test Method for Determining Air Change in a Single Zone by Means of a Tracer Gas Dilution*. West Conshohocken, PA, US.

Augenbroe, Godfried. 2002. "Trends in Building Simulation." *Building and Environment* 37 (8–9): 891–902. doi:10.1016/S0360-1323(02)00041-0.

Clarke, J A. 2001. *Energy Simulation in Building Design 2nd Edition*. Book. Butterworth-Heinemann.

Cole, Wesley J., Kody M. Powell, Elaine T. Hale, and Thomas F. Edgar. 2014. "Reduced-Order Residential Home Modeling for Model Predictive Control." *Energy and Buildings* 74 (2014): 69–77.

Crawley, Drury B., Jon W. Hand, Michaël Kummert, and Brent T. Griffith. 2008. "Contrasting the Capabilities of Building Energy Performance Simulation Programs." *Building and Environment* 43 (4): 661–673.

Dawson-Haggerty, Stephen, Xiaofan Jiang, Gilman Tolle, and David E. Culler. 2010. "SMAP - A Simple Measurement and Actuation Profile for Physical Information." In *Proceedings of the 8th International Conference on Embedded Networked Sensor Systems, SenSys 2010, November 3-5, 2010*. Zurich, Switzerland.

Deru, Michael, Kristin Field, Daniel Studer, Kyle Benne, Brent Griffith, Paul Torcellini, Bing Liu, et al. 2011. *U . S . Department of Energy Commercial Reference Building Models of the National Building Stock*.

DOE. 2015. *EnergyPlus Engineering Reference: The Reference to EnergyPlus Calculations*.

DOE. 2016. "EnergyPlus." https://energyplus.net/.

Hong, Tianzhen, S.K Chou, and T.Y Bong. 2000. "Building Simulation: An Overview of Developments and Information Sources." *Building and Environment* 35 (4): 347–361.

Hong, Tianzhen, Mary Ann Piette, Yixing Chen, Sang Hoon Lee, Sarah C. Taylor-Lange, Rongpeng Zhang, Kaiyu Sun, and Phillip Price. 2015. "Commercial Building Energy Saver: An Energy Retrofit Analysis Toolkit." *Applied Energy* 159: 298–309.

Hunn, Bruce D. 1996. *Fundamentals of Building Energy Dynamics*. MIT Press.

ISO. 2008. "ISO 13790: 2008 Energy Performance of Buildings —Calculation of Energy Use for Space Heating and Cooling." Report.

ISO. 2012. *Thermal Performance of Buildings and Materials – Determination of Specific Airflow Rate in Buildings — Tracer Gas Dilution Method, 12569:2012*. Geneva, Switzerland.

Kokogiannakis, Georgios, Paul Strachan, and Joe Clarke. 2008. "Comparison of the Simplified Methods of

the ISO 13790 Standard and Detailed Modelling Programs in a Regulatory Context." Journal Article. *Journal of Building Performance Simulation* 1 (4): 209–219.

LBNL. 2016. "FLEXLAB The World's Most Advanced Building Efficiency Test Bed." https://flexlab.lbl.gov/.

Lee, Sang Hoon, Tianzhen Hong, Mary Ann Piette, Geof Sawaya, Yixing Chen, and Sarah C. Taylor-Lange. 2015. "Accelerating the Energy Retrofit of Commercial Buildings Using a Database of Energy Efficiency Performance." *Energy* 90: 738–747.

Wang, Shengwei, and Xinhua Xu. 2006. "Parameter Estimation of Internal Thermal Mass of Building Dynamic Models Using Genetic Algorithm." *Energy Conversion and Management* 47 (13–14): 1927–1941.

Zeng, Ruolang, Xin Wang, Hongfa Di, Feng Jiang, and Yinping Zhang. 2011. "New Concepts and Approach for Developing Energy Efficient Buildings: Ideal Specific Heat for Building Internal Thermal Mass." *Energy and Buildings* 43 (5). Elsevier B.V.: 1081–1090.

Zhang, Yuna, Zheng O'Neill, Bing Dong, and Godfried Augenbroe. 2015. "Comparisons of Inverse Modeling Approaches for Predicting Building Energy Performance." *Building and Environment* 86 (2015): 177–190.

Zhao, Hai Xiang, and Frédéric Magoulès. 2012. "A Review on the Prediction of Building Energy Consumption." *Renewable and Sustainable Energy Reviews* 16 (6): 3586–3592.